Krzysztof Ludwinek, Jan Staszak, Tomasz Bekier, Jarosław Kurkiewicz
Kielce University of Technology

INFLUENCE OF FIELD CURRENT WAVEFORM ON HIGHER HARMONIC CONTENT IN CYLINDRICAL SYNCHRONOUS GENERATOR

Abstract: The paper presents a comparison of the higher harmonics in the induced voltages in the stator windings of cylindrical synchronous generator rated at 8.5 kVA under no-load conditions. The comparison is made for the generator with linear and non-linear magnetic circuit without damping cage using constant and variable field current. The calculations of the electromagnetic parameters are carried out in FEMM program. The simulation results are verified experimentally.

1. Introduction

Linearity and non-linearity of the magnetic circuit with inhomogeneous air gap of the synchronous generator have a decisive impact on the distribution of the magnetic field in the air gap and the shape of the induced stator voltage [1-6]. The occurrence of harmonics in induced stator voltage in synchronous generator is also determined by the type of stator windings (in synchronous generators of low power up to tens of kVA most commonly used winding is a single layer winding) [7], damping bar influence [8, 9], rotor or stator skew [9, 10], voltage or field current control method [7, 10] and the stator or rotor eccentricity [11, 12].

In salient pole synchronous generators much more irregular shape of the air gap (compared to cylindrical generators) means that both the magnetic field and induced phase voltage are significantly distorted by third harmonic [4, 5, 7, 8]. Occurrence of the third harmonic is the result of magnetic circuit's non-linearity and the concentrated nature of field winding in two wide slots around the circumference of the rotor per pair of poles and per stator winding. Even in synchronous generator with skewed rotor there is an insignificant change of third harmonic (in the magnetic field and induced voltages) because the influence of rotor or stator skew on lower order harmonics reduction is small [7, 13].

In cylindrical synchronous generator the shape of the magnetic field in an air gap is more regular (than in the salient pole synchronous generator) due to initial uniformity of the air gap between the stator teeth and the rotor teeth. In order to minimize induced phase voltage distortion the span of the central wide tooth of the rotor is selected so that its shape is as close to the trapezoid as possible [14].The current linkage $F(x)$ of such rotor can be expressed as:

$$F(x)=\frac{4A}{\pi\alpha}\left(\sin\alpha\sin x+\frac{\sin 3\alpha}{3^2}\sin x+\frac{\sin 5\alpha}{5^2}\sin x+\ldots\right) \quad (1)$$

where the: A – linkage amplitude.

For linear magnetic circuit, if the inclination angle of the side of the trapezoid equals $\alpha=2\pi/3$ the third harmonic disappears. For non-linear magnetic circuit even for $\alpha=2\pi/3$ the third harmonic is present but with a lower amplitude than in the salient pole synchronous generator.

2. Model of a cylindrical synchronous generator

Due to the presence of higher harmonics in the inductance distributions in the *dq0*-axes it is easier to carry out induced stator voltages calculations with a circuit model of a cylindrical synchronous generator in the stator and rotor natural reference frame [13].

Figure 1 shows the equivalent circuit parameters of a cylindrical generator in the stator and rotor natural reference frame under no-load conditions. The equivalent circuit represents the stator windings and the field winding [15].

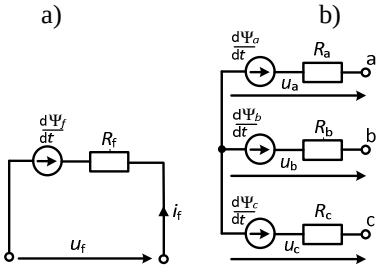

Fig. 1. Equivalent circuit parameters of a cylindrical synchronous generator under no-load conditions a) field winding, b) stator windings

Based on an equivalent circuit of cylindrical synchronous generator (Fig. 1) the induced voltages can be derived from the equations in stator coordinates (for stator windings) and in rotor coordinates (for rotor windings) [15].

$$\left.\begin{aligned} u_a &= \frac{d\Psi_a(\theta,i)}{dt} \\ u_b &= \frac{d\Psi_b(\theta,i)}{dt} \\ u_c &= \frac{d\Psi_c(\theta,i)}{dt} \end{aligned}\right\} \tag{2}$$

$$u_f = \omega\frac{\partial\Psi_f(\theta,i)}{\partial\theta}i_f + R_f i_f \tag{3}$$

where: a, b, c – indexes of stator windings, f – field winding index, Ψ_a, Ψ_b, Ψ_c – stator linkage fluxes, u_a, u_b, u_c – stator phase voltages.

As the equation (2) demonstrates the induced phase voltages are described by the derivative of the flux coupled with stator windings. Taking into account the impact of field current and electrical angle of the rotor's position (θ) changes, the derivative can be expressed as follows [6]:

$$\frac{d\boldsymbol{\Psi}(\theta,i)}{dt} = \frac{d\theta}{dt}\frac{\boldsymbol{\Psi}(\theta,i)}{\partial\theta} + \frac{\partial\boldsymbol{\Psi}(\theta,i)}{\partial i}\frac{d\mathbf{i}}{dt} \tag{4}$$

Figure 2 shows the relationship between induced line-to-line voltage as a function of field current under no-load conditions. The no-load characteristics of examined 8.5 kVA cylindrical synchronous generator are obtained experimentally in laboratory measurement set.

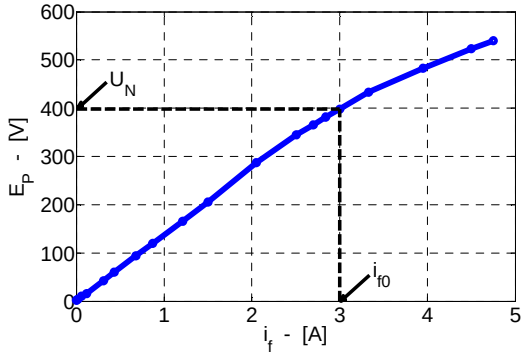

Fig 2. Line-to-line voltage as a function of field current under no-load conditions

As shown in Figure 2, the generator works on the linear part of the characteristic so the equation (4) can be simplified to [6, 18]:

$$\frac{d\boldsymbol{\Psi}(\theta)}{dt} = \frac{d\theta}{dt}\frac{\partial\mathbf{L}(\theta)}{\partial\theta}\mathbf{i} + \mathbf{L}(\theta)\frac{d\mathbf{i}}{dt} \tag{5}$$

Based on equations (5) and (2) and taking into account the mutual inductance distributions between stator and rotor windings as well as the self-inductance of stator windings the induced phase voltage can be expressed in a following manner:

$$\mathbf{u}_s = \omega\frac{\partial\mathbf{L}_{sf}(\theta)}{\partial\theta}i_f + \mathbf{L}_{sf}(\theta)\frac{di_f}{dt} \tag{6}$$

And consequently field windings voltage:

$$u_f = R_f i_f + \omega\frac{\partial L_f(\theta)}{\partial\theta}i_f + \mathrm{L}_f(\theta)\frac{di_f}{dt} \tag{7}$$

where: $\mathbf{u}_s = [u_a, u_b, u_c]^{\mathrm{T}}$ – matrix of induced stator phase voltages, $\mathbf{L}_{sf} = [L_{af}, L_{bf}, L_{cf}]^{\mathrm{T}}$ – matrix of mutual inductances between stator and rotor windings, i_f – field current, R_f – resistance of field winding.

From the equation (6) the induced stator phase voltages can be derived:

$$\left.\begin{aligned} u_a &= \omega\frac{\partial L_{af}(\theta)}{\partial\theta}i_f + L_{af}(\theta)\frac{di_f}{dt} \\ u_b &= \omega\frac{\partial L_{bf}(\theta)}{\partial\theta}i_f + L_{bf}(\theta)\frac{di_f}{dt} \\ u_c &= \omega\frac{\partial L_{cf}(\theta)}{\partial\theta}i_f + L_{cf}(\theta)\frac{di_f}{dt} \end{aligned}\right\} \tag{8}$$

In case of $i_f = I_f = const$ the equation (8) can be expressed as

$$\left.\begin{aligned} u_a &= \omega\frac{\partial L_{af}(\theta)}{\partial\theta}i_f \\ u_b &= \omega\frac{\partial L_{bf}(\theta)}{\partial\theta}i_f \\ u_c &= \omega\frac{\partial L_{cf}(\theta)}{\partial\theta}i_f \end{aligned}\right\} \tag{9}$$

3. Determination of the higher harmonic content

Parameters of the investigated cylindrical synchronous generator are computed using FEMM 2D software [16, 17]. Figure 3 presents distribution of magnetic field lines of the generator as computed by FEMM.

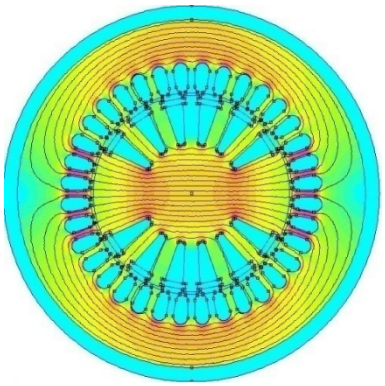

Fig. 3. Magnetic flux distribution in the 8.5 kVA cylindrical synchronous generator with nonlinear magnetic circuit

Figure 4 presents induced stator phase voltages (I_f = const).

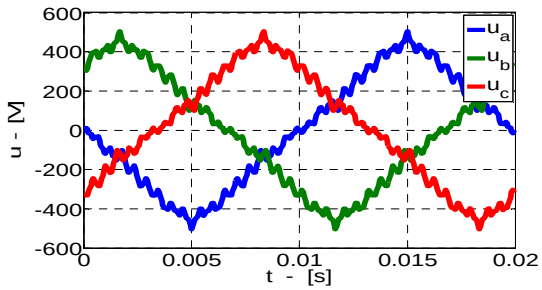

Fig. 4. Induced stator voltages in case of I_f = const and linear magnetic circuit

Figure 5 presents induced voltages assuming U_f = const and a linear magnetic circuit.

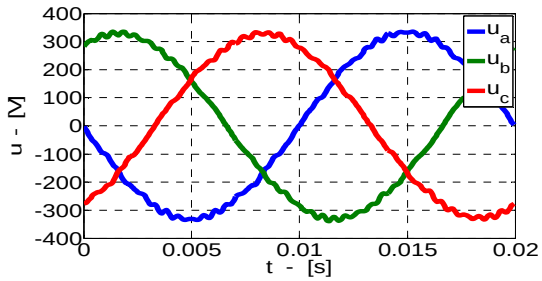

Fig. 5. Induced stator phase voltages assuming U_f = const and a linear magnetic circuit

In this particular cases (I_f = const – Fig. 4 and U_f = const – Fig. 5) there are only subtle differences between linear and nonlinear magnetic circuit which can be seen in Figure 6.

a)

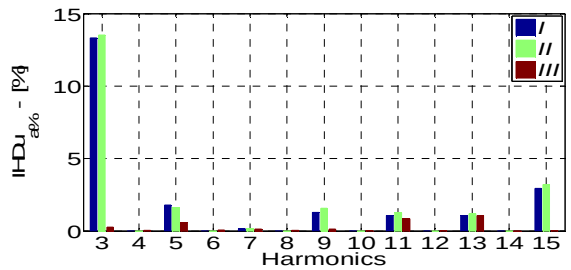

b)

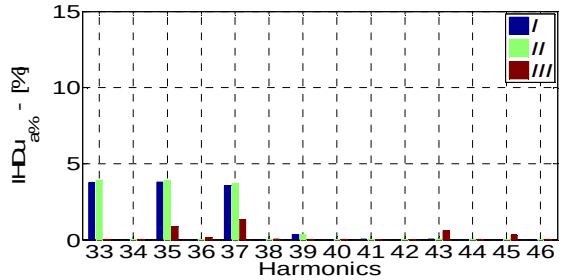

c)

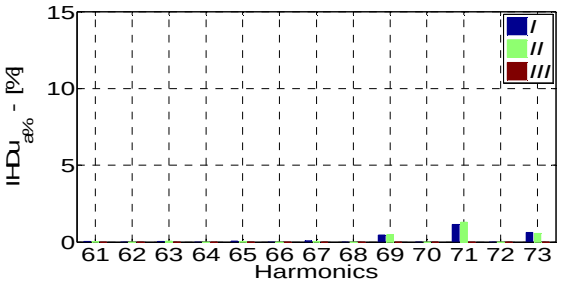

*Fig. 6. Comparison of the harmonic content in induced single phase voltage: a) from 2nd to the 15th order, b) from 33rd to 46th order), c) 61st to 73rd order, **I** - I_f = const and linear magnetic circuit, **II** - I_f = const and non-linear magnetic circuit, **III** - U_f = const, linear and nonlinear magnetic circuit*

For both I_f = const cases the presented higher harmonic content analysis demonstrated a significant influence of 3rd and 15th harmonics. Beside slotting harmonics (35th, 37th, 71st, 73rd stator slotting harmonics as well as 11th and 13th rotor slotting harmonics) there is a significant distortion caused by 9th and 33rd harmonics. In case of U_f = const, 9th, 33rd, 69th, 71st, and 73rd harmonics disappear and 3rd, 5th, 15th, 35th and 37th are significantly diminished.

Total Harmonic Distortion factor ($THDu_{a\%}$) is determined in order to compare higher harmonic content in induced voltages. Table 1 presents a $THDu_{a\%}$ comparison for analyzed cases.

*Tab. 1. Comparison of the total harmonic distortion in induced phase voltage: **I** - I_f = const, linear magnetic circuit, **II** - I_f = const, non-linear magnetic circuit, **III** - U_f = const, linear magnetic circuit*

$THDu_{a\%}$ (***I***)	$THDu_{a\%}$ (***II***)	$THDu_{a\%}$ (***III***)
15.51 %	15.89 %	2.44 %

Based on the above results it can be concluded that U_f = const model is characterized by much lower harmonic content in induced voltages.

4. Experimental verification

Figure 7 presents the measurement set used for experimental verification of simulation results. The cylindrical synchronous generator with the following rating is used: S_N = 8,5 kVA, U_N = 400 V, I_N = 15,25 A, n_N = 3000 rpm, $cos\varphi_N$ = 0,85.

During experimental investigation the field winding is supplied from a DC voltage source and the induced voltages as well as field current waveforms are registered using Tektronix 3014 Mixed Signal Oscilloscope.

a)

b)

Fig. 7. View of a) measurement set, b) examined cylindrical synchronous generator

Figure 8 demonstrates induced voltages as registered by the oscilloscope.

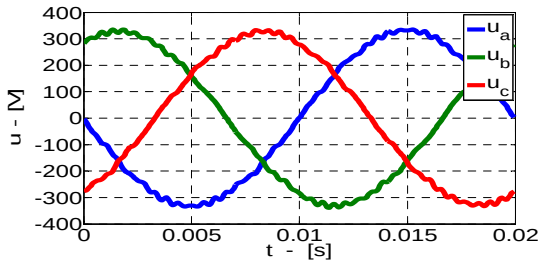

Fig. 8. Registered waveforms of the induced stator voltages under no-load conditions of the cylindrical synchronous generator

In Figure 9 the field current waveform is presented under no-load conditions of the examined cylindrical synchronous generator.

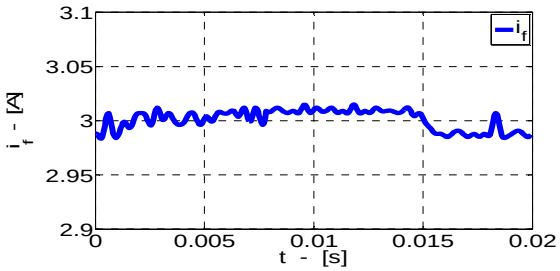

Fig. 9. Registered waveforms of field current under no-load conditions

By introducing the registered field current waveform into expression (8) and applying appropriate transformations it is possible to determine chosen equation parameters such as $\omega \frac{\partial L_{sf}}{\partial \Theta} i_f$ and $L_{sf} \frac{di_f}{dt}$

Figure 10 presents a comparison of aforementioned factors for a single phase *a* of investigated generator and their influence on the induced voltage shape.

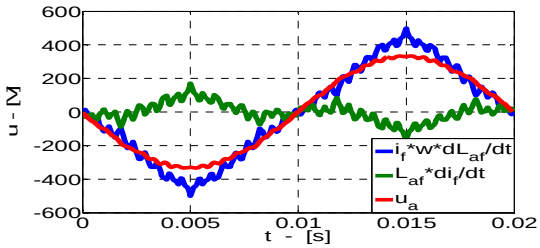

Fig. 10. Influence of two components in (8) on the shape of the waveform of induced single phase voltage

IHDu% and *THDu*% parameters are computed in order to compare experimental results with the simulation. Figure 11 demonstrates harmonic content of the 3 registered phase voltages.

a)

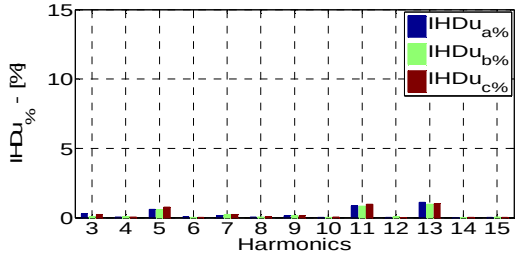

b)

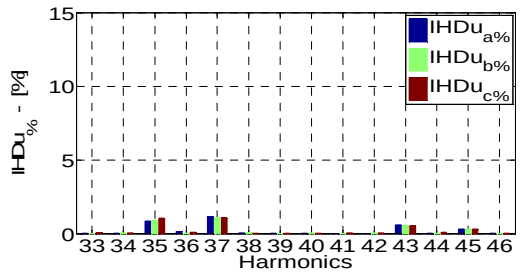

c)

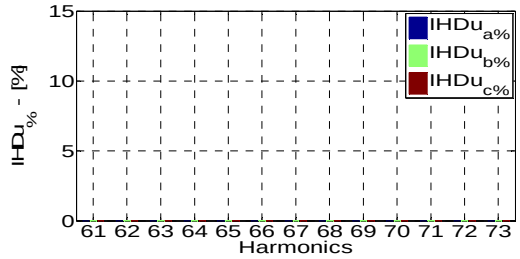

Fig. 11. Harmonic content of the registered waveform of the induced stator phase voltages: a) from 2nd to the 15th harmonic, b) from 33rd to 46th c) 61st to 73rd harmonics

As can be concluded from the presented analysis there are no significant differences between registered voltages and those derived from U_f = const simulation model. Consequently $THDu_{\%}$ comparison yields similar results as can be seen in Table 2.

Tab. 2. Total harmonic content in registered waveform of the induced stator phase voltage

$THDu_{a\%}$	$THDu_{b\%}$	$THDu_{c\%}$
2.35 %	2.18 %	2.39 %

5. Conclusion

The influence of nonlinearity on induced stator phase voltages is rather small in the presented cylindrical synchronous generator model and can be safely discarded. It is a direct result of utilization of an oversized stator which is rated at 22 kW. Simplification of mixed field-circuit computations by assuming constant field current yields vastly different results compared to experimental ones. As can be seen beside slotting harmonics (35th, 37th, 71st, 73rd) there is a significant influence of 3rd, 5th, 9th, 15th and 33rd harmonics. Their presence is a result of assuming constant field current. In case of supplying the field winding with $U_f = const$, components $\omega\frac{\partial L_{af}}{\partial \vartheta}i_f$ and $\frac{di_f}{dt}L_{af}$, $\omega\frac{\partial L_{bf}}{\partial \vartheta}i_f$ and $\frac{di_f}{dt}L_{bf}$, $\omega\frac{\partial L_{cf}}{\partial \vartheta}i_f$ and $\frac{di_f}{dt}L_{cf}$ are not in counterphase. This is due to the fact that $\frac{di_f}{dt}L_{af}$, $\frac{di_f}{dt}L_{bf}$ and $\frac{di_f}{dt}L_{cf}$ are equal to zero and consequently the induced stator voltages have much greater total higher harmonic contents $THDu_{a\%}$ (15.51% and 15.89% with linear and nonlinear magnetic circuit, respectively) than in case of U_f = const where $THDu_{a\%}$ is equal to 2.44% from simulation and is less than 2.40% from experimental investigation.

Bibliography

[21]. Z. Eleschova, A. Belan, M. Mucha "Harmonic Distortion Produced by Synchronous Generator in Thermal -Power Plant", *Proceedings of the 6th WSEAS International Conference on Power Systems*, September 22-24, Lisbon, Portugal, 2006.

[22]. J. Moreira, T. A. Lipo: *Modeling of Saturated AC Machines Including Airgap Flux Harmonic Components*, IEEE-IAS Conference Record, Oct. 7-12, 1990, Part 1, pp. 37-44.

[23]. J. Bernatt, S. A. Gawron, M. Glinka "Experimental Validation of Hybrid Excited Permanent Magnet Synchronous Generator", *Przegląd elektrotechniczny, No 12a*, pp. 66-70, 2012,

[24]. T. J. Sobczyk, A. Warzecha "*Alternative approaches to modelling of electrical machines with nonlinear magnetic circuit*", *Archives of Electrical Engineering*, Vol. 46, No 1, pp. 421-434, 1997.

[25].T. J. Sobczyk "Extreme Possibilities of Circuital Models of Electric Machines", *Electrical Power Quality and Utilisation*, Vol. 7, No. 2, pp. 103 – 110, 2006.

[26]. I. Boldea "Synchronous generators", *CRC Press Taylor &Francis Group*, 2006.

[27]. K. Ludwinek "Influence of DC voltage and current of field winding on induced stator voltages of a salient pole synchronous generator", *International Review of Electrical Engineering* (I.R.E.E.), Vol. 9, No. 1, pp. 62-72, 2014.

[28]. S. Wiak, R. Nadolski, K. Ludwinek, J. Staszak "Influence of the Synchronous Cylindrical Machine Damping Cage on Content of Higher Harmonics in Armature Currents During Co-Operation with the Distorted and Asymmetrical Electric Power System", *Computer Engineering in Applied Electromagnetism*, (IOS Press, 2006, 520 – 527).

[29]. K. Ludwinek "Proposed way of modeling the damping circuits on the rotor of a salient pole synchronous generator" (in Polish), Zeszyty Problemowe Maszyny Elektryczne, No. 104, Wydawnictwo Komel Katowice, Poland, pp. 179-186, 2014.

[30]. D. Chaudhary, A. Kumar, S. M.Chauhan "Analysis of Harmonic Free Voltage Regulator with Simulation Technique". *International Journal of Emerging Trends in Electrical and Electronics* (IJETEE), Vol. 9, No. 1, pp. 18-22, 2013.
[31]. K. Weinreb, T. Węgiel, M. Sułowicz "Influence of inside asymmetry in asynchronous motor on spectrum of stator currents", *Proceeding of XLIInd International Symposium on Electrical machines* SME'2006, 3-6 July, Cracow, pp. 307 – 310, 2006.
[32]. K. Weinreb, M. Sułowicz, A. Dziechciarz: Application of instantaneous power for rotor eccentricity detection in synchronous motor, *Zeszyty Problemowe Maszyny Elektryczne* published by Komel Katowice, No. 104, pp. 301-306, 2014.
[33]. K. Ludwinek "Some aspects of representation of inductance distributions in dq0-axes in a salient pole synchronous generator", *Zeszyty Problemowe Maszyny Elektryczne* published by Komel Katowice, no. 104, Poland, pp. 187-184, 2014.
[34]. J. Pyrhönen, T. Jokinen, V. P. Hrabcová "Design of rotating electrical machines", *John Wiley & Son*s, 2014.
[35]. K. Ludwinek "Representation of the stator to rotor self- and mutual inductances in a salient pole synchronous generator in the no-load state", *Zeszyty Problemowe - Maszyny Elektryczne* published by Komel Katowice, No. 104, Poland, pp. 147-154, 2014.
[36]. Finite Element Method Magnetics: Octave-FEMM. Version 1.0. User's Manual, 2006.
[37]. http://www.femm.info/wiki/HomePage.

Author's information

Krzysztof Ludwinek PhD, k.ludwinek@tu.kielce.pl
Jan Staszak PhD DSc, j.staszak@tu.kielce.pl
Tomasz Bekier MSc, tbekier@tu.kielce.pl
Jarosław Kurkiewicz MSc, jkurkiewicz@tu.kielce.pl
Kielce University of Technology,
Faculty of Electrical Engineering, Automatic Control and Computer Science,
Al. Tysiąclecia PP. 7, 25–314 Kielce, Poland